

# Velocity dependence of baryon screening in a hot strongly coupled plasma

---

**Christiana Athanasiou, Hong Liu and Krishna Rajagopal**

*Center for Theoretical Physics, Massachusetts Institute of Technology,  
Cambridge, MA 02139, USA*

*E-mail addresses:* `athanasi@mit.edu`, `hong_liu@mit.edu`, `krishna@ctp.mit.edu`

**ABSTRACT:** The  $L$ -dependence of the static potential between  $N_c$  quarks arranged in a circle of radius  $L$  (a “baryon”) immersed in the hot plasma of a gauge theory with  $N_c$  colors defines a screening length  $L_s$ . We use the AdS/CFT correspondence to compute this screening length for the case of heavy quarks in the plasma of strongly coupled  $\mathcal{N} = 4$  super Yang-Mills theory moving with velocity  $v$  relative to the baryon. We find that in the  $v \rightarrow 1$  limit,  $L_s \propto (1 - v^2)^{1/4}/T$ , and find that corrections to this velocity dependence are small at lower velocities. This result provides evidence for the robustness of the analogous behavior of the screening length defined by the static quark-antiquark pair, which has been computed previously and in QCD is relevant to quarkonium physics in heavy ion collisions. Our results also show that as long as the hot wind is not blowing precisely perpendicular to the plane of the baryon configuration that we analyze, the  $N_c$  different quarks are not all affected by the wind velocity to the same degree, with those quarks lying perpendicular to the wind direction screened most effectively.

**KEYWORDS:** AdS/CFT correspondence, Thermal Field Theory.

---

## Contents

1. Introduction and Summary	1
2. General baryon configurations	6
3. Velocity dependence of baryon screening in $\mathcal{N} = 4$ SYM theory	10
3.1 Wind perpendicular to the baryon configuration	10
3.2 Wind parallel to the baryon configuration	16
4. Discussion	22

---

## 1. Introduction and Summary

The simplest example of the AdS/CFT correspondence is provided by the duality between  $\mathcal{N} = 4$  supersymmetric Yang-Mills (SYM) theory and classical gravity in  $\text{AdS}_5 \times \text{S}_5$  [1].  $\mathcal{N} = 4$  super Yang-Mills theory is a conformally invariant theory with two parameters: the rank of the gauge group  $N_c$  and the 't Hooft coupling  $\lambda = g_{\text{YM}}^2 N_c$ . In the large  $N_c$  and large  $\lambda$  limit, gauge theory problems can be solved using classical gravity in  $\text{AdS}_5 \times \text{S}_5$  geometry. We shall work in this limit throughout this paper.

In  $\mathcal{N} = 4$  SYM theory at zero temperature, the static potential between a heavy external quark and antiquark separated by a distance  $L^{\text{meson}}$  is given in the large  $N_c$  and large  $\lambda$  limit by [2, 3]

$$V(L) = -\frac{4\pi^2}{\Gamma(\frac{1}{4})^4} \frac{\sqrt{\lambda}}{L^{\text{meson}}}, \quad (1.1)$$

where the  $1/L^{\text{meson}}$  behavior is required by conformal invariance. This potential is obtained by computing the action of an extremal string world sheet, bounded at  $r \rightarrow \infty$  ( $r$  being the fifth dimension of  $\text{AdS}_5$ ) by the world lines of the quark and antiquark and “hanging down” from these world lines toward smaller  $r$ . At nonzero temperature, the potential becomes [4]

$$\begin{aligned} V(L^{\text{meson}}, T) &\approx \sqrt{\lambda} f(L^{\text{meson}}) & L^{\text{meson}} < L_c^{\text{meson}} \\ &\approx \lambda^0 g(L^{\text{meson}}) & L^{\text{meson}} > L_c^{\text{meson}}. \end{aligned} \quad (1.2)$$

In (1.2), at  $L_c^{\text{meson}} = 0.24/T$  there is a change of dominance between different saddle points and the slope of the potential changes discontinuously. When  $L^{\text{meson}} < L_c^{\text{meson}}$ , the potential is determined

as at zero temperature by the area of a string world sheet bounded by the worldlines of the quark and antiquark, but now the world sheet hangs down into a different five-dimensional spacetime: introducing nonzero temperature in the gauge theory is dual to introducing a black hole horizon in the five-dimensional spacetime. When  $L^{\text{meson}} \ll L_c^{\text{meson}}$ ,  $f(L^{\text{meson}})$  reduces to its zero temperature behavior (1.1). When  $L^{\text{meson}} > L_c^{\text{meson}}$ , the potential arises from two disjoint strings, each separately extending downward from the quark or antiquark all the way to the black hole horizon. At  $L^{\text{meson}} \gg L_c^{\text{meson}}$ ,  $g(L^{\text{meson}})$  is known and is determined by the exchange of the lightest supergravity mode between the two disjoint strings [5]. It is physically intuitive to interpret  $L_c$  as the screening length  $L_s$  of the plasma since at  $L_c$  the qualitative behavior of the potential changes. Similar criteria are used in the definition of screening length in QCD [6], although in QCD there is no sharply defined length scale at which screening sets in. Lattice calculations of the static potential between a heavy quark and antiquark in QCD indicate a screening length  $L_s \sim 0.5/T$  in hot QCD with two flavors of light quarks [7] and  $L_s \sim 0.7/T$  in hot QCD with no dynamical quarks [8]. The fact that there is a sharply defined  $L_c$  in (1.2) is an artifact of the limit in which we are working.

In Refs. [9, 10], the analysis of screening was extended to the case of a quark-antiquark pair moving through the plasma with velocity  $v$ . In that context, it proved convenient to define a slightly different screening length  $L_s^{\text{meson}}$ , which is the  $L^{\text{meson}}$  beyond which no connected extremal string world sheet hanging between the quark and antiquark can be found. At  $v = 0$ ,  $L_s^{\text{meson}} = 0.28/T$  [4]. At nonzero  $v$ , up to small corrections that have been computed [9, 10],

$$L_s^{\text{meson}}(v, T) \simeq L_s^{\text{meson}}(0, T)(1 - v^2)^{1/4} \propto \frac{1}{T}(1 - v^2)^{1/4}. \quad (1.3)$$

This result, also obtained in Ref. [11] and further explored in Refs. [13–15], has proved robust in the sense that it applies in various strongly coupled plasmas other than  $\mathcal{N} = 4$  SYM [13–15]. (See Refs. [16] for other recent work.) The velocity dependence of the screening length (1.3) suggests that in a theory containing dynamical heavy quarks and meson bound states (which  $\mathcal{N} = 4$  SYM does not) the dissociation temperature  $T_{\text{diss}}(v)$ , defined as the temperature above which mesons with a given velocity do not exist, should scale with velocity as [9]

$$T_{\text{diss}}(v) \simeq T_{\text{diss}}(v = 0)(1 - v^2)^{1/4}, \quad (1.4)$$

since  $T_{\text{diss}}(v)$  should be the temperature at which the screening length  $L_s^{\text{meson}}(v)$  is comparable to the size of the meson bound state. The scaling (1.4) indicates that slower mesons can exist up to higher temperatures than faster ones. This result has proved robust in a second sense, in that (1.4) has also been obtained by direct analysis of the dispersion relations of actual mesons in the plasma [17, 18], introduced by adding heavy quarks described in the gravity dual by a D7-brane whose fluctuations are the mesons [19]. These mesons have a limiting velocity whose temperature dependence is equivalent to (1.4) [18], up to few percent corrections that have been computed [18].

In the present paper, we shall return to the velocity-dependent screening length and test the robustness of (1.3) in yet a third sense, by analyzing the potential and screening length defined by a configuration consisting of  $N_c$  external quarks arranged in a circle of radius  $L$ .<sup>1</sup> In the gravity

<sup>1</sup>The baryon static potential between three static quarks has been computed in QCD itself using lattice methods at zero temperature [20], and very recently the extension of these studies to nonzero temperatures and hence the study of baryon screening in QCD has been initiated [21].

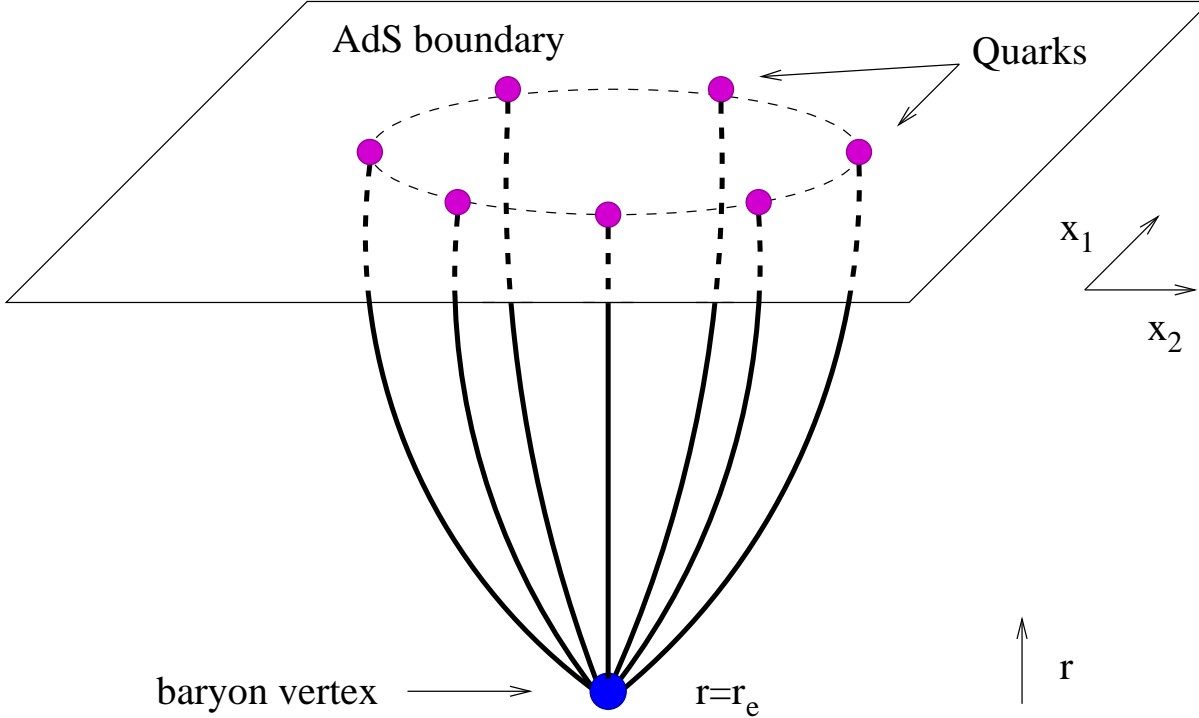


**Figure 1:** A sketch of a baryon configuration with  $N_c$  quarks arranged in a circle at the boundary of the AdS space, each connected to a D5-brane located at  $r = r_e$  by a string.

dual, there is a string hanging down from each of these quarks and at nonzero  $T$  and large enough  $L$ , the only extremal configuration of these string world sheets will be  $N_c$  disjoint strings. In order to obtain a baryon-like configuration, we introduce a D5-brane into the gravity dual theory which fills the 5 spatial dimensions of the  $S_5$  and sits at a point in  $\text{AdS}_5$ , and on which  $N_c$  strings can end [22–24].<sup>2</sup> This now means that for  $L$  less than some  $L_s$  we can find configurations as in Fig. 1, in which the  $N_c$  strings hanging down from the quarks at the boundary of  $\text{AdS}_5$  end on the D5-brane. Following Ref. [24], we have made the arbitrary choice of placing the  $N_c$  quarks in a circle; pursuing

<sup>2</sup>We shall only consider the case where all  $N_c$  strings are located at the same point in the  $S_5$ ; it would be interesting to generalize our analysis to the case where there are different species of quarks corresponding to strings located at different points in the  $S_5$  which could then end at different points on the D5-brane. We are also neglecting the interactions between the  $N_c$  string endpoints on the D5-brane. Such interactions can be described via the Born-Infeld action for the D5-brane, and have been analyzed in Refs. [25] for the case where the baryons are BPS objects and the analysis can be pushed through to completion. In our case, in which supersymmetry is broken by the nonzero temperature and in which the baryon configurations need not be BPS objects even at zero temperature, such an analysis certainly presents technical challenges and may even be made uncontrolled by potential higher derivative corrections to the D5-brane Born-Infeld action. We shall follow Refs. [22–24] in neglecting string-string interactions. We shall find that the velocity dependence of the screening length is controlled by the kinematics of the AdS black hole metric under boosts: the fact that we find (see below) the same velocity dependence for the screening length defined by a baryon configuration which includes a D5-brane as has been found previously for that defined by the quark-antiquark potential whose calculation involves no D5-brane suggests, but absent a calculation does not demonstrate, that the addition of string-string interactions on the D5-brane will not modify our conclusions.

our analysis to the point of phenomenology would certainly require investigating more generalized configurations.<sup>3</sup> Our central purpose, however, is to test the robustness of (1.3) in a theoretical context in which the D5-brane introduces a qualitatively new element. Note that in comparing our results for baryon screening to (1.3), if we want to compare numerical prefactors we should compare  $L$  to  $L^{\text{meson}}/2$ , since we have defined  $L$  as the radius of the circle in Fig. 1 rather than its diameter.

The D5-brane plays a role somewhat analogous what has been called a “baryon-junction” in various phenomenological analyses of baryons in QCD [26]. Baryon junctions in phenomenological analyses have usually been envisioned as well localized in (3+1)-dimensions, but this may not be the appropriate way of thinking of the D5-brane. The IR/UV relationship that characterizes the AdS/CFT correspondence [27] tells us that smaller values of the fifth-dimension coordinate  $r$  correspond to larger length scales  $R^2/r$  in the (3+1)-dimensional field theory, where  $R$  is the curvature of the AdS space. The D5-brane is located at  $r = r_e$ , the lowest point in  $r$  of any part of the baryon configuration in Fig. 1. It therefore represents the longest wavelength “disturbance” of the (3+1)-dimensional gluon field (and other  $\mathcal{N} = 4$  SYM fields) caused by the presence of the  $N_c$  quarks. We shall see in Section 3 that in  $\mathcal{N} = 4$  SYM this length scale  $R^2/r_e$  is comparable to  $2L$ , meaning that the baryon vertex describes a disturbance of the gluon fields comparable in size to the circle of external quarks, not a baryon junction that is localized in (3+1)-dimensions.

The results (1.3) and (1.4) have a simple physical interpretation which suggests that they could be applicable to a wide class of theories regardless of specific details. First, note that since  $L_s(0) \sim \frac{1}{T}$ , both (1.3) and (1.4) can be interpreted as if in their rest frame the quark-antiquark dipole experiences a higher effective temperature  $T\sqrt{\gamma}$ . Although this is not literally the case in a weakly coupled theory, in which the dipole will see a redshifted momentum distribution of quasiparticles coming at it from some directions and a blueshifted distribution from others [28], we give an argument below for how this interpretation can nevertheless be sensible. The result (1.3) can then be seen as validating the relevance of this interpretation in a strongly coupled plasma. The argument is based on the idea that quarkonium propagation and dissociation are mainly sensitive to the local energy density of the medium. Now, in the rest frame of the dipole, the energy density  $\varepsilon$  is blue shifted by a factor  $\sim \gamma^2$  and since  $\varepsilon \propto T^4$  in a conformal theory, the result (1.3) is as if quarks feel a higher effective temperature given by  $T\sqrt{\gamma}$ . Lattice calculations indicate that the quark-gluon plasma in QCD is nearly conformal over a range of temperatures  $1.5T_c < T \lesssim 5T_c$ , with an energy density  $\varepsilon \approx bT^4$  where  $b$  is approximately constant, at about 80% of the free theory value [30]. So it does not seem far-fetched to imagine that (1.3) could apply to QCD. We should also note that AdS/CFT calculations in other strongly coupled gauge theories with a gravity description are consistent with the interpretation above [14, 18] and that for near conformal theories the deviation from conformal theory behavior appears to be small [14]. If a velocity scaling like (1.3) and (1.4) holds for QCD, it can potentially have important implications for quarkonium suppression in heavy

---

<sup>3</sup>Note that for  $N_c = 3$ , there is no loss of generality in choosing the  $N_c$  quarks to lie in a single plane, but there is still an infinite space of distinct possible configurations to consider. Many have been considered in lattice investigations [20, 21]. It would also be worthwhile to extend our analysis to treatments of baryons themselves, rather than simply calculating the screening length defined by a particular (in our case circular) configuration of  $N_c$  quarks. Such an analysis would not directly address the question we pose, namely the robustness of the velocity dependence of screening, but it would certainly be a significant step toward actual baryon phenomenology. The methods developed in Refs. [25] could provide a good starting point.

ion collisions [9, 18], in particular suggesting that in a heavy ion collision at RHIC (or LHC) which does not achieve a high enough temperature to dissociate  $J/\Psi$  (or  $\Upsilon$ ) mesons at rest, the production of these quarkonium mesons with transverse momentum above some threshold may nevertheless be suppressed [9].<sup>4</sup> Our results suggest that if baryons containing three charm quarks are ever studied in heavy ion collision experiments, the suppression of their production could be similarly dependent on transverse momentum.

In Section 2 we shall set up a general formalism for finding baryon configurations of heavy external quarks in supergravity, with the  $N_c$  quarks arranged arbitrarily. In Section 3 we shall apply this general formalism to the configuration depicted in Fig. 1, allowing us to define a screening length  $L_s$ . In Section 3.1 we evaluate  $L_s(v, T)$  for the case where the baryon configuration is moving through the plasma in a direction perpendicular to the plane defined by the circle of quarks. (Equivalently, the ‘‘baryon’’ feels a plasma wind blowing in a direction perpendicular to its plane.) Static configurations are found by extremizing the total baryon action coming from both the strings and the D5 brane. We find static configurations only for  $L < L_s(v, T)$  with  $L_s(0, T) = 0.094/T$  as in [24], comparable to  $\frac{1}{2}L^{\text{meson}}(0, T)$  above, and with

$$L_s(v, T) = \frac{0.083}{T}(1 - v^2)^{1/4} \quad (1.5)$$

in the  $v \rightarrow 1$  limit. In this limit, we obtain (1.5) analytically. We find numerically that  $L_s(v, T)/(1 - v^2)^{1/4}$  varies monotonically and smoothly from 0.094 at  $v = 0$  to 0.083 at  $v \rightarrow 1$ , making

$$L_s(v, T) \simeq L_s(0, T)(1 - v^2)^{1/4} \quad (1.6)$$

a good approximation. In Section 3.2 we do a similar numerical calculation for the case where the wind velocity is parallel to the baryon’s plane. At high velocities we find a result like (1.5) except that the proportionality constant is different for different quarks/strings, depending weakly on the angle between the wind velocity and the string.  $L_s$  is smallest for the quarks whose strings are oriented perpendicular to the wind, even though in the configuration that we analyze these quarks are also closest to the D5-brane. This indicates that as  $v$  increases the medium is most effective at screening the potential felt by these quarks.

---

<sup>4</sup>These phenomenological implications rest as much on the analysis of the velocity dependence of screening, introduced in [9] for mesons and generalized here to baryons, as they do on the construction of the dispersion relations of the mesons themselves as in [18]. The dispersion relations extend to arbitrarily large wave vectors: there is a limiting velocity but, for  $\lambda \rightarrow \infty$ , no limiting momentum. At finite  $\lambda$ , the mesons have nonzero widths [18]; if these widths grow with increasing meson momentum, this could serve to limit the meson momenta also [31]. In the absence of widths, as for  $\lambda \rightarrow \infty$ , inferences about meson production rely upon the observation that the potential between a quark and antiquark moving with high enough velocity is screened, making it unlikely that they will bind into a meson even though a slowly moving meson state with the same momentum as the quark and antiquark pair does exist [18]. Thus, if we are to use a baryon analysis to test the robustness of phenomenological conclusions drawn in the meson sector, a key point to test is the velocity dependence of screening. Doing so, as in this paper, does not require analysis of the dissociation of actual baryons.

## 2. General baryon configurations

We wish to analyze a baryon configuration of  $N_c$  heavy external quarks in the  $\mathcal{N} = 4$  SYM plasma at nonzero temperature. The baryon construction in supergravity involves  $N_c$  fundamental strings with the same orientation, beginning at the heavy quarks on the AdS boundary and ending on the baryon vertex in the interior of  $\text{AdS}_5$ , which is a D5 brane wrapped on the  $S_5$  [22]. In this Section, we shall allow the  $N_c$  quarks to be placed at arbitrary positions in the  $(x_1, x_2, x_3)$ -space at the boundary of AdS. Note that the  $\mathcal{N} = 4$  SYM plasma contains no particles in the fundamental representation, so the quarks we study here are external.

The gravity theory dual to  $\mathcal{N} = 4$  SYM theory at nonzero temperature is the AdS black hole times a five-dimensional sphere, with the metric

$$ds^2 = -f(r)dt^2 + \frac{r^2}{R^2}d\bar{x}^2 + \frac{dr^2}{f(r)} + R^2d\Omega_5^2, \quad (2.1)$$

where

$$f(r) = \frac{r^2}{R^2} \left(1 - \frac{r_0^4}{r^4}\right). \quad (2.2)$$

Here,  $d\Omega_5^2$  is the metric for a unit  $S_5$ ,  $R$  is the curvature radius of the AdS metric,  $r$  is the coordinate of the fifth dimension of  $\text{AdS}_5$  and  $r_0$  is the position of the black hole horizon. The temperature of the gauge theory is given by the Hawking temperature of the black hole,  $T = r_0/(\pi R^2)$ . And, the gauge theory parameters  $N_c$  and  $\lambda$  are given by  $\sqrt{\lambda} = R^2/\alpha'$  and  $\lambda/N_c = g_{\text{YM}}^2 = 4\pi g_s$  where  $1/(2\pi\alpha')$  is the string tension and  $g_s$  is the string coupling constant. (So, large  $N_c$  and  $\lambda$  correspond to large string tension and weak string coupling and thus justify the classical gravity treatment.)

We shall always work in the rest frame of the baryon configuration. This means that in order to describe  $N_c$  quarks moving through the plasma with velocity  $v$ , say in the  $x_3$ -direction, we must boost the metric (2.1) such that it describes a  $\mathcal{N} = 4$  SYM plasma moving with a wind velocity  $v$  in the negative  $x_3$ -direction. We obtain

$$ds^2 = -Adt^2 + 2Bdt dx_3 + Cdx_3^2 + \frac{r^2}{R^2}(dx_1^2 + dx_2^2) + \frac{1}{f(r)}dr^2 + R^2d\Omega_5^2, \quad (2.3)$$

where

$$A = \frac{r^2}{R^2} \left(1 - \frac{r_1^4}{r^4}\right), \quad B = \frac{r_1^2 r_2^2}{r^2 R^2}, \quad C = \frac{r^2}{R^2} \left(1 + \frac{r_2^4}{r^4}\right), \quad (2.4)$$

with

$$r_1^4 = r_0^4 \cosh^2 \eta, \quad \text{and} \quad r_2^4 = r_0^4 \sinh^2 \eta. \quad (2.5)$$

We have defined the wind rapidity  $\eta$  via  $v = -\tanh \eta$ . Although in Section 3 we shall specialize to circular baryon configurations as illustrated in Fig. 1, in this Section we describe the construction of a baryon configuration with  $N_c$  heavy external quarks placed at arbitrary locations  $(x_1, x_2, x_3)$  at  $r \rightarrow \infty$  in the boosted AdS metric (2.3).

The construction in this Section can easily be generalized to baryon configurations a large class of gauge theories at nonzero temperature, including  $\mathcal{N} = 4$  SYM as one example. Consider any

gauge theory that is dual in the large  $N_c$  and strong coupling limit to Type IIB string theory in the supergravity approximation in a generic string frame metric that can be written in the form

$$ds^2 = g_{\mu\nu}(r)dx^\mu dx^\nu + \frac{dr^2}{f(r)} + e^{2\psi(r)}ds_5^2, \quad (2.6)$$

with the possibility of a nontrivial dilaton  $\phi(r)$ . As before,  $x^\mu = (t, \vec{x}) = (t, x_1, x_2, x_3)$  describe the Yang-Mills theory coordinates (the boundary coordinates). Here,  $ds_5^2$  is the metric of some five-dimensional compact manifold  $M_5$  that may not be  $S_5$ . A specific choice of gauge theory will correspond to specific choices of  $\phi(r)$  and the various metric functions appearing in (2.6). The metric (2.6) is not even the most general that we could analyze, since for example we have not allowed the metric functions in (2.6) to depend on the coordinates of the internal manifold  $M_5$  and since we have chosen the  $r$ -dependence of the  $M_5$ -metric to be a common factor  $\exp(2\psi(r))$ , not some more complicated structure. Such complications do not add qualitatively new features to the analysis of baryon configurations in a metric of the form (2.6). Our construction of baryon configurations below starting from the metric (2.6) could be applied to gauge theories known to have dual gravity descriptions some of which are conformal and some not, without or with nonzero  $R$ -charge density, with  $\mathcal{N} = 4$  supersymmetry or to certain theories with only  $\mathcal{N} = 2$  or  $\mathcal{N} = 1$  supersymmetry, at nonzero or zero temperature, with or without a wind velocity. In our explicit definition of and calculation of the screening length  $L_s$  in Section 3, we shall return to the special case (2.3) of hot  $\mathcal{N} = 4$  SYM theory with a wind velocity.

A baryon configuration in the supergravity metric (2.6) involves  $N_c$  fundamental strings beginning at the external heavy quarks on the boundary (which we will take to be at  $r = \infty$ ) and ending on the baryon vertex in the interior, which is a D5 brane wrapped on the compact manifold  $M_5$  [22]. We denote the positions in  $\vec{x}$ -space where we place the external quarks by  $\vec{q}^{(a)}$ , with  $a = 1, \dots, N_c$ , and we take all the quarks to sit at the same point in the compact manifold  $M_5$ . We shall describe how to determine the location of the D5-brane below. After so doing, we shall shift the origin of the  $\vec{x}$  coordinates such that the D5-brane sits at the origin, at  $\vec{x}_e = 0$ . We denote its position in the fifth dimension by  $r = r_e$ . The total action of the system is then given by

$$S_{\text{total}} = \sum_{a=1}^{N_c} S_{\text{string}}^{(a)} + S_{\text{D5}}, \quad (2.7)$$

where  $S_{\text{string}}^{(a)}$  denotes the action of the fundamental string connecting the  $a$ -th quark with the D5-brane. Denoting the string worldsheet coordinates  $(\tau, \sigma)$ , we can choose

$$\tau = t, \quad \sigma = r, \quad x_i = x_i(\sigma), \quad (2.8)$$

meaning that the shape of the  $a$ 'th string worldsheet is described by functions  $x_i^{(a)}(r)$  that extend from  $\vec{x}^{(a)}(r_e) = \vec{x}_e$  to  $\vec{x}^{(a)}(\infty) = \vec{q}^{(a)}$ . The Nambu-Goto action of one string can then be written as

$$S_{\text{string}} = \frac{\mathcal{T}}{2\pi\alpha'} \int_{r_e}^{\infty} dr \sqrt{-\frac{g_{00}}{f} + (g_{0i}g_{0j} - g_{00}g_{ij}) x'_i x'_j} \equiv \frac{\mathcal{T}}{2\pi\alpha'} \int dr \mathcal{L}_{\text{string}}, \quad (2.9)$$

where  $\mathcal{T}$  is the total time and where  $x'_i \equiv \partial_r x_i$ . The action for the five-brane can be written as

$$S_{\text{D5}} = \frac{\mathcal{V}(r_e) \mathcal{T} V_5}{(2\pi)^5 \alpha'^3}, \quad \mathcal{V}(r) = \sqrt{-g_{00}} e^{-\phi+5\psi}, \quad (2.10)$$

where  $V_5$  is the volume of the compact manifold  $M_5$  and  $\mathcal{V}(r_e)$  can be considered to be the gravitational potential for the D5-brane located at  $r = r_e$ .

In order to find a static baryon configuration, we must extremize  $S_{\text{total}}$ , first with respect to the functions  $x_i^{(a)}(r)$  that describe the trajectories of each of the  $N_c$  strings and second with respect to  $\vec{x}_e$  and  $r_e$ , the location of the D5-brane. Because  $S_{\text{total}}$  does not depend on the  $x_i^{(a)}(r)$  explicitly, the variation with respect to  $x_i^{(a)}(r)$  leads to Euler-Lagrange equations that have a first integral

$$\frac{\partial \mathcal{L}_{\text{string}}^{(a)}}{\partial x_i'^{(a)}} = \frac{(g_{0i}g_{0j} - g_{00}g_{ij}) x_j'^{(a)}}{\mathcal{L}_{\text{string}}^{(a)}} = \text{const.} \equiv K_i^{(a)}, \quad (2.11)$$

where we have denoted the integration constants by  $K_i^{(a)}$ . Next, we extremize the action with respect to variations in the position of the D5-brane, understanding that as we vary its position we adjust the string trajectories as required by their Euler-Lagrange equations. Extremizing the action with respect to the location of the D5-brane in  $\vec{x}$ -space yields equations which receive one contribution from the boundary term at the D5-brane at  $r = r_e$  in the variation of each of the  $x_i^{(a)}(r)$ , equations which take the form

$$\sum_a K_i^{(a)} = 0. \quad (2.12)$$

(What arises from the variation are the  $K_i^{(a)}$  evaluated at  $r = r_e$ , but the  $K_i^{(a)}$  are by construction  $r$ -independent.) The constraint (2.12) is a force balance condition, encoding the requirement that in a static baryon configuration the net force exerted by the  $N_c$  strings on the D5-brane in the  $x_i$  directions, with  $i = 1, 2$  and  $3$ , must vanish. Extremizing  $S_{\text{total}}$  with respect to  $r_e$  yields the  $r$ -direction force balance condition which we can write as

$$\sum_{a=1}^{N_c} H^{(a)} \Big|_{r_e} = \Sigma, \quad (2.13)$$

where

$$H^{(a)} \equiv \mathcal{L}^{(a)} - x_i'^{(a)} \frac{\partial \mathcal{L}^{(a)}}{\partial x_i'^{(a)}} = \frac{-g_{00}}{f(r) \mathcal{L}_{\text{string}}^a} \quad (2.14)$$

is the “upward” (i.e. in the positive  $r$ -direction) force on the D5-brane from the  $a$ ’th string, meaning that the left-hand side of (2.13) is the upward force due to all the strings, and where

$$\Sigma \equiv \frac{2\pi\alpha'}{\mathcal{T}} \frac{\partial S_{\text{D5}}}{\partial r_e} = \frac{V_5}{(2\pi)^4 \alpha'^2} \frac{\partial \mathcal{V}(r_e)}{\partial r_e} \quad (2.15)$$

is the downward gravitational force on the D5-brane, given its placement at  $r = r_e$  in the curved spacetime (2.6). Including the contribution to the energy from the interaction among the  $N_c$  string endpoints on the D5-brane (which has been calculated in simpler settings than ours [25]) would affect our calculation only by modifying this downward force somewhat.

Eqs. (2.11), (2.12) and (2.13) determine the shape of the string trajectories and the location of the D5-brane, which is to say that they determine the baryon configuration for a given choice of the positions of the quarks  $\vec{q}^{(a)}$ . Used in this way, one would integrate the first order equations (2.11), using the boundary conditions  $\vec{x}^{(a)}(\infty) = \vec{q}^{(a)}$  to determine the integration constants  $\vec{K}^{(a)}(\vec{q}^{(a)}, \vec{x}_e, r_e)$  for a given choice of  $\vec{x}_e$  and  $r_e$ . Eqs. (2.12) and (2.13) can then be used to determine  $\vec{x}_e$  and  $r_e$ . Not all choices of  $\vec{q}^{(a)}$  will yield a static baryon configuration. For a given quark distribution at the boundary, the question of whether equations (2.11), (2.12) and (2.13) have solutions is a dynamical question depending on the specific metric under consideration. We shall see specific examples of how this plays out in Section 3.

Alternatively, a baryon configuration can be specified by starting with a set of  $\vec{K}^{(a)}$  satisfying (2.12), solving for  $r_e$  using (2.13), and integrating Eqs. (2.11) outward from  $r = r_e$  to the boundary at  $r = \infty$ , only then learning the quark positions  $\vec{q}^{(a)}$  in the gauge theory. Instead of specifying  $\vec{K}^{(a)}$ , one can equivalently specify  $\vec{s}^{(a)} \equiv \partial_r \vec{x}^{(a)}(r)|_{r=r_e}$ .

Whether we think of specifying conditions at  $r = r_e$  and integrating inwards or specifying conditions at the D5-brane, since we are considering the  $N_c \rightarrow \infty$  limit it is often more convenient to introduce the density of quarks and strings instead of discrete position variables. At the boundary, the quark configuration can be specified by a density of quarks  $\rho(\vec{q})$ , which can be normalized as

$$\int d^3 \vec{q} \rho(\vec{q}) = 1. \quad (2.16)$$

We can then rewrite (2.12) as

$$\int d^3 \vec{q} \rho(\vec{q}) \vec{K}(\vec{q}) = 0. \quad (2.17)$$

However, (2.13) cannot immediately be written in terms of  $\rho(\vec{q})$  because the quantities in (2.13) are evaluated at  $r = r_e$ , and unlike the  $K$ 's occurring in (2.12) are not  $r$ -independent. So, we must use the string trajectories themselves to relate the density of quarks at  $r = \infty$  to a density of strings at  $r = r_e$ , as follows. For any given  $r_e$  and  $\vec{x}_e$ , a solution  $\vec{x}(r)$  to Eqs. (2.11) describes a single string trajectory which connects a particular point  $\vec{q}$  at  $r = \infty$  to the D5-brane at  $\vec{x}(r_e) = \vec{x}_e$ . The string connects to the D5-brane with a particular value of the “angle”  $\vec{s} = \partial_r \vec{x}(r)|_{r=r_e}$ . So, the set of string trajectories  $\vec{x}(r)$  with all possible choices of  $\vec{q}$  determine a mapping from  $\vec{q}$  onto  $\vec{s}$ , where the  $\vec{q}$ 's specify the location of quarks at infinity and the  $\vec{s}$ 's specify strings at the D5-brane. Since the mapping corresponds to Hamiltonian “time” evolution (with  $r$  playing the role of time) Liouville's theorem tells us that a given  $\rho(\vec{q})$  maps onto a  $\rho_V(\vec{s})$  that specifies the density of strings hitting the D5-brane as a function of angle given by

$$\rho_V(\vec{s}) = \rho(\vec{q}) \left| \frac{\partial (q_1, q_2, q_3)}{\partial (s_1, s_2, s_3)} \right|. \quad (2.18)$$

In evaluating the Jacobian determinant, the  $\vec{q}$ 's should be considered to be functions of the  $\vec{s}$ 's, with the function being the mapping defined by the string trajectories  $\vec{x}(r)$ . If the solutions  $\vec{x}(r)$  are nontrivial curved trajectories, then the relation between  $\rho(\vec{q})$  and  $\rho_V(\vec{s})$  will be nontrivial. Eqs. (2.12) and (2.13) can now be recast in terms of  $\rho_V(\vec{s})$ , namely<sup>5</sup>

$$\int d^3\vec{s} \rho_V(\vec{s}) \vec{K}(\vec{s}) = 0 \quad (2.19)$$

and

$$\int d^3\vec{s} \rho_V(\vec{s}) H(\vec{s}) = \frac{\Sigma}{N_c} . \quad (2.20)$$

Note that  $\vec{K}(\vec{s})$  is obtained by evaluating the left hand side of (2.11) at  $r = r_e$ , while  $H(\vec{s})$  is obtained by evaluating equation (2.14) at  $r = r_e$ .

We close this Section with a description of one way in which the formalism that we have developed can be used. Suppose that we wish to describe a baryon configuration in which the quarks all lie on some closed two dimensional surface in  $\vec{x}$ -space. For a given  $r_e$ , we can then use (2.12) in the form (2.17) to determine the density of quarks along the surface required for any choice of  $\vec{x}_e$  located inside the surface. Or, if the density of quarks along the surface has been specified, we can use (2.12) to determine  $\vec{x}_e$  for a given  $r_e$ . We then repeat this exercise for all values of  $r_e$  until we find an  $r_e$  that satisfies (2.13) in the form (2.20).

In next Section we apply (2.11), (2.12) and (2.13) to particular baryon configurations in a  $\mathcal{N} = 4$  SYM plasma moving with a nonzero wind velocity.

### 3. Velocity dependence of baryon screening in $\mathcal{N} = 4$ SYM theory

We now refocus on baryon configurations at rest in the plasma of  $\mathcal{N} = 4$  SYM theory with temperature  $T$  moving with a wind velocity  $v = -\tanh \eta$  in the  $x_3$  direction. The gravity dual of this hot plasma wind is described by the metric (2.3). Following Ref. [24], we shall analyze baryon configurations in which the  $N_c$  quarks all lie in a single plane. In Section 3.1 we take the quarks to be uniformly distributed along a circle in the  $(x_1, x_2)$ -plane, perpendicular to the direction of the wind. In Section 3.2 we analyze a configuration in which the quarks lie in the  $(x_1, x_3)$ -plane, parallel to the direction of the wind. We expect that the two configurations we shall study are sufficient to illustrate the generic aspects of the velocity dependence of baryon screening in  $\mathcal{N} = 4$  SYM theory.

#### 3.1 Wind perpendicular to the baryon configuration

In this subsection we consider a baryon configuration lying in the  $(x_1, x_2)$ -plane (i.e.  $x_3 = 0$ ) perpendicular to the wind direction. For simplicity, we arrange the  $N_c$  external quarks uniformly

---

<sup>5</sup>Note that in the continuous limit,

$$\frac{1}{N} \sum_a (\dots) \rightarrow \int d^3\vec{s} \rho_V(\vec{s}) (\dots) = \int d^3\vec{q} \rho(\vec{q}) (\dots) .$$

around a circle of radius  $L$  as in [24], see Fig. 1. This is a simple example within which we can illustrate many aspects of the general formalism of Section 2 for constructing baryon configurations, and define and study the velocity dependence of the screening length.

With the quarks arranged uniformly around a circle, it is clear by symmetry that the D5-brane must sit at the center of the circle, which we shall take to be at the origin:  $\vec{x}_e = 0$ . Because of the rotational symmetry of the circular configuration and of the background geometry (2.3), each of the  $N_c$  strings in Fig. 1 is equivalent. They all sit at  $x_3 = 0$ , and each can be described by a single function  $x(r)$ , where  $x \equiv \sqrt{x_1^2 + x_2^2}$  extends from  $x = 0$  and  $r = r_e$ , at the D5-brane, to  $x = L$ , at the boundary of  $\text{AdS}_5$ . With the D5-brane at  $\vec{x}_e = 0$  at the center of the circle, it is clear that the forces in the  $\vec{x}$  directions exerted by the strings on the D5-brane cancel, meaning that Eqs. (2.12) are automatically satisfied. The D5-brane sits at some  $r = r_e$ , which we shall determine for a given  $L$  using (2.13). So,  $x(r_e) = 0$  and  $x(\infty) = L$ . Applying equations (2.9) and (2.10) to (2.3), we find that in this case

$$\mathcal{L}_{\text{string}} = \sqrt{A \left( \frac{(x')^2 r^2}{R^2} + \frac{1}{f(r)} \right)}, \quad (3.1)$$

and

$$S_{\text{D5}} = \frac{N_c \mathcal{T} R \sqrt{A(r_e)}}{8\pi\alpha'}, \quad (3.2)$$

where  $f(r)$  and  $A(r)$  were given in Eqs. (2.2), (2.4) and (2.5). The equation (2.11) that determines the shape of the string trajectory  $x(r)$  becomes

$$\frac{A r^2 x'}{R^2 \mathcal{L}_{\text{string}}} = K, \quad (3.3)$$

where by symmetry there is only a single integration constant  $K$  for all the strings. The  $r$ -direction force balance condition (2.13), namely the condition that the upward force on the D5-brane exerted by the  $N_c$  strings balances the downward force of gravity, becomes

$$\left. \frac{A}{f \mathcal{L}_{\text{string}}} \right|_{r_e} = \frac{1 + \rho^4 \cosh^2 \eta}{4\sqrt{1 - \rho^4 \cosh^2 \eta}} \equiv \Sigma(\rho, \eta), \quad (3.4)$$

where we have defined

$$\rho \equiv \frac{r_0}{r_e} = \frac{\pi R^2 \mathcal{T}}{r_e}. \quad (3.5)$$

We must solve (3.3) and (3.4) simultaneously, in so doing obtaining both the position of the D5-brane  $r_e$  and the shape of the strings  $x(r)$  corresponding to a static baryon configuration with size  $L$ .

The integration constant  $K$  must be the same at any  $r$ . Upon evaluating it at  $r = r_e$  and after some algebraic manipulations, equations (3.3) and (3.4) can be written more explicitly as

$$x' = \frac{K}{\sqrt{\left( A \frac{r^2}{R^2} - K^2 \right) \frac{r^2}{R^2} f(r)}}, \quad (3.6)$$

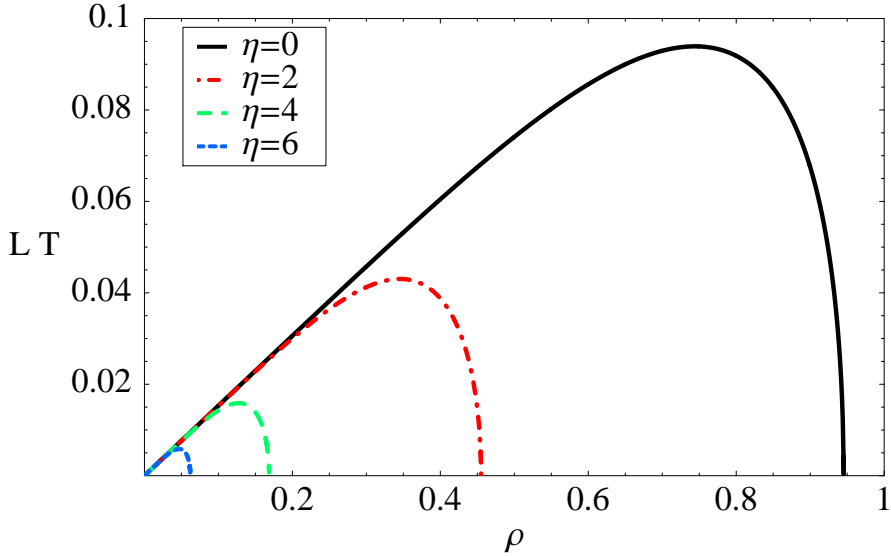


**Figure 2:** Baryon radius  $L$  versus  $\rho$ , where  $\rho = r_0/r_e$  is the ratio of the position of the black hole horizon to the position of the D5-brane, for several different values of the rapidity  $\eta$  of the hot wind. The screening length  $L_s$  at a given  $\eta$  is the maximum of  $L(\rho)$ , namely the largest  $L$  at which a static baryon configuration can be found. We see that  $L_s$  decreases with increasing wind velocity.

and

$$\frac{K^2 R^4}{r_e^4} = 1 - \rho^4 \cosh^2 \eta - (1 - \rho^4) \Sigma^2, \quad (3.7)$$

from which we obtain an explicit expression for the baryon radius  $L$  in terms of  $\rho$  and the rapidity  $\eta$ :

$$L = \frac{\rho}{\pi T} (1 - \rho^4 \cosh^2 \eta - (1 - \rho^4) \Sigma^2)^{\frac{1}{2}} \int_1^\infty dy \frac{1}{(y^4 - \rho^4)^{\frac{1}{2}} (y^4 - 1 + (1 - \rho^4) \Sigma^2)^{\frac{1}{2}}}, \quad (3.8)$$

where  $y \equiv r/r_e$ . We have evaluated (3.8) numerically, and in Fig. 2 we plot  $L$  versus  $\rho$  for several values of  $\eta$ . We see that  $L$  is small when  $\rho$  is small (meaning that  $r_e$  is large). As we decrease  $r_e$ , pulling the D5-brane in Fig. 1 downward,  $\rho$  increases and the size of the baryon configuration  $L$  at first increases, then reaches a maximum value, and then decreases to zero. For a given  $\eta$ , therefore, there is a maximum possible baryon radius, which we denote  $L_s$ , beyond which no baryon configurations are found. We shall identify  $L_s$  with the screening length, although in so doing we neglect a small correction that we shall discuss below. We see from Fig. 2 that at any  $\eta$  for  $L < L_s(\eta)$  there are two solutions with different values of  $\rho$ . We shall see below that the configuration with the larger  $\rho$  is unstable and has a higher energy.

According to (3.8), the nonzero value of  $\rho$  at which  $L \rightarrow 0$  in Fig. 2 is the  $\rho$  at which the right-hand side of (3.7) vanishes. At this value of  $\rho$ ,  $K$  is zero and  $\partial_r x|_{r_e} = 0$ , corresponding to a configuration whose strings have become vertical. Note that the D5-brane becomes heavier when it is closer to the AdS black hole (i.e.  $\Sigma$  in (3.4) increases with  $\rho$ ), meaning that the strings emerging from the D5-brane must be more and more vertical in order to hold it at rest. At some  $\rho$ , the strings

become vertical and at larger  $\rho$  (smaller  $r_e$ ) no static configuration can be found. From (3.7) we also see that this largest possible  $\rho$  is always smaller than the  $\rho = 1/\sqrt{\cosh \eta}$  at which the speed  $v$  exceeds the local speed of light at the position of the D5-brane.

At any  $L$  for which there are two string configurations possible in Fig. 2, we expect that the solution with the larger  $\rho$  is unstable, as in the case of the string configuration between a quark and antiquark [29]. This instability can be seen on qualitative grounds as follows. For the solutions with smaller  $\rho$ , we see from Fig. 2 that  $L$  increases monotonically with  $\rho$ . This means that if we deform the configuration by pulling the D5-brane downward while keeping  $L$  fixed, the deformed configuration with its enlarged  $\rho$  has too small an  $L$  to be static. The fact that  $L$  “wants” to be larger means that the upward force on the D5-brane is greater than required to balance the downward force of gravity. So, there is a net restoring force pulling the D5-brane back upwards and the original configuration is stable against this deformation. In contrast, for the solutions with larger  $\rho$  we see from Fig. 2 that  $L$  decreases monotonically with  $\rho$ , meaning that if we pull the D5-brane downward,  $L$  “wants” to be smaller and the upward force on the D5-brane is less than the downward force of gravity (the downward force has increased more than the upward force) and the D5-brane will accelerate downward. The configurations described by the part of the curve in Fig. 2 for which  $L$  decreases with increasing  $\rho$  are therefore unstable. We shall see below that these configurations have higher energy than the stable configurations with the same  $L$  and smaller  $\rho$ .

We can use (3.8) and Fig. 2 to compare the length scale  $R^2/r_e$  of the disturbance of the gluon field induced by the  $N_c$  external quarks to  $2L$ , the size of the circle of quarks itself. In the small- $\rho$  limit, (3.8) simplifies to

$$LT \approx \frac{0.4811 \rho}{\pi}, \quad (3.9)$$

which describes the linear region seen in all of the curves in Fig. 2 at small  $\rho$ . This implies that at small  $\rho$

$$\frac{R^2}{r_e} \approx 2.079 L, \quad (3.10)$$

comparable to  $2L$ . We see from Fig. 2 that as we go from this small  $\rho$  regime towards  $L = L_s$ , the ratio of  $R^2/r_e$  to  $2L$  increases by a further few tens of percent.

We see from Fig. 2 that the screening length  $L_s$  decreases with increasing velocity. At zero velocity,  $L_s = 0.094/T$  as can be obtained from previous results [24]. We have evaluated  $L_s$  as a function of rapidity  $\eta$ , and shall plot the result in Fig. 7, along with analogous results from Section 3.2 for the case where the wind velocity is parallel to the plane of the baryon configuration. From our numerical evaluation, we find that at large  $\eta$

$$L_s \approx \frac{a}{T\sqrt{\cosh \eta}}, \quad (3.11)$$

with  $a = 0.0830$ . The screening length for a quark and antiquark separated by a distance  $L^{\text{meson}}$  moving through the plasma in a direction perpendicular to the dipole also takes the form (3.11) in the high velocity limit, with  $a = 0.237$  [9]. When we compare the  $L_s$  that we have computed for the baryon configuration to  $L_s^{\text{meson}}/2$  (the “radius” of the meson configuration at its screening

length) we see that, in addition to having precisely the same velocity dependence at high velocity, their numerical values are comparable. Finally, it is perhaps not surprising that  $L_s^{\text{baryon}}$  is somewhat smaller than  $L_s^{\text{meson}}/2$ , for a given  $\eta$  and  $T$ , since the baryon vertex (D5-brane) pulls the strings further downward, closer to the horizon.

We can also find the large  $\eta$  dependence of  $L_s$  analytically. If we define

$$\hat{\rho} \equiv \rho \sqrt{\cosh \eta}, \quad \hat{L} \equiv L \sqrt{\cosh \eta} \quad (3.12)$$

and take the scaling limit in which

$$\eta \rightarrow \infty \quad \text{with} \quad \hat{\rho}, \quad \hat{L} \quad \text{held fixed}, \quad (3.13)$$

we find that  $\cosh \eta$  drops out of the leading terms in Eq. (3.8) and this equation becomes

$$\begin{aligned} \hat{L} &= \frac{\hat{\rho}}{\pi T} (1 - \hat{\rho}^4 - \Sigma^2)^{\frac{1}{2}} \int_1^\infty dy \frac{1}{y^2 (y^4 - 1 + \Sigma^2)^{\frac{1}{2}}} + O\left((\cosh \eta)^{-\frac{1}{2}}\right) \\ &= \frac{\hat{\rho}}{3\pi T} (1 - \hat{\rho}^4 - \Sigma^2)^{\frac{1}{2}} {}_2F_1\left(\frac{1}{2}, \frac{3}{4}, \frac{7}{4}, 1 - \Sigma^2\right) + O\left((\cosh \eta)^{-\frac{1}{2}}\right). \end{aligned} \quad (3.14)$$

(Note that according to (3.4),  $\Sigma$  only depends on  $\hat{\rho}$ .) The right-hand side of (3.14) is function of  $\hat{\rho}$  that goes to zero at  $\hat{\rho} \rightarrow 0$  and at  $\hat{\rho} \rightarrow 0.880$ , and that has a maximum at  $\hat{\rho} = 0.666$  where  $\hat{L} = 0.0830/T$ , yielding an  $L_s$  that is in precise agreement with (3.11).

We close this section by evaluating the energy of the baryon configurations that we have constructed. The energy of one string can be found using  $S_{\text{string}}$  and is given by

$$\begin{aligned} E_{\text{string}} &= \frac{1}{2\pi\alpha'} \int_{r_e}^\infty dr \sqrt{A \left( \frac{(x')^2 r^2}{R^2} + \frac{1}{f} \right)} \\ &= \frac{T\sqrt{\lambda}}{2\rho} \int_1^\infty dy \frac{y^4 - \rho^4 \cosh^2 \eta}{(y^4 - \rho^4)^{\frac{1}{2}} (y^4 - 1 + (1 - \rho^4)\Sigma^2)^{\frac{1}{2}}}, \end{aligned} \quad (3.15)$$

where  $y \equiv r/r_e$ . This energy is infinite because we have included the masses of the quarks. As in Refs. [9, 10], we regularize the baryon energy by subtracting the energy of (in this case  $N_c$ ) disjoint quarks in a hot plasma wind of velocity  $v$ , whose strings are dragging behind them in the  $x_3$  direction according to the solution found in [12, 32]. This corresponds to regulating the  $r$ -integral in (3.15) with a large- $r$  cutoff  $\Lambda$ , subtracting

$$E_{\text{mass}} = \frac{N_c}{2\pi\alpha'} \int_{r_0}^\Lambda dr = \frac{N_c T \sqrt{\lambda}}{2\rho} \int_\rho^{\Lambda/r_e} dy, \quad (3.16)$$

and then taking  $\Lambda$  to infinity. This procedure yields a finite answer. The total energy of the baryon (strings plus D5-brane) becomes

$$\begin{aligned} E_{\text{total}} &= \frac{N_c T \sqrt{\lambda}}{2} \left[ \frac{1}{\rho} \int_1^\infty dy \left( \frac{y^4 - \rho^4 \cosh^2 \eta}{(y^4 - \rho^4)^{\frac{1}{2}} (y^4 - 1 + (1 - \rho^4)\Sigma^2)^{\frac{1}{2}}} - 1 \right) + 1 - \frac{1}{\rho} \right. \\ &\quad \left. + \frac{\sqrt{1 - \rho^4 \cosh^2 \eta}}{4\rho} \right], \end{aligned} \quad (3.17)$$

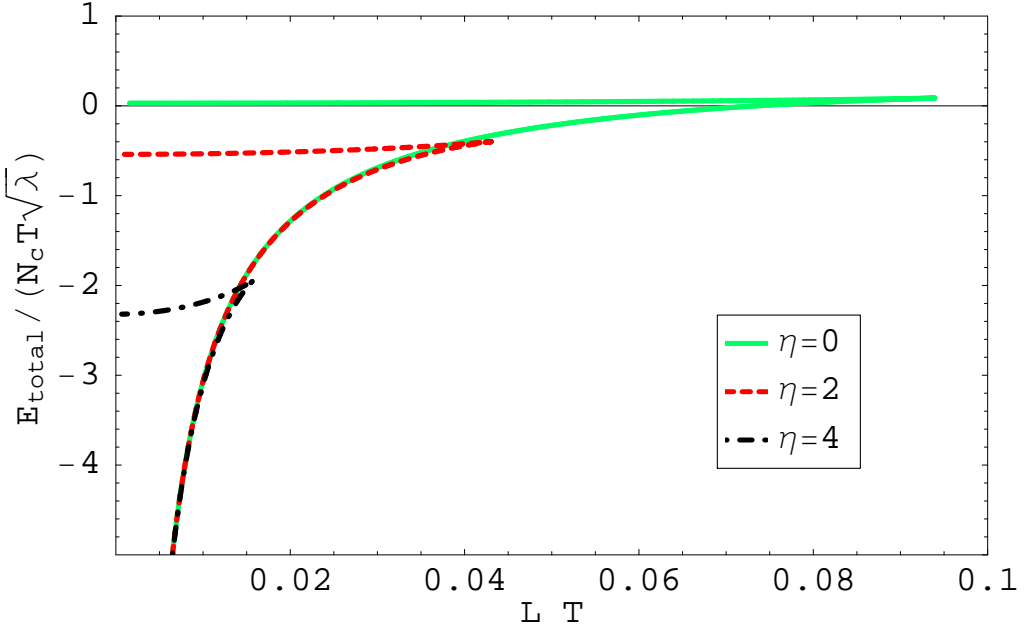


**Figure 3:** The total energy of the baryon configuration with a given  $L$  (relative to that of  $N_c$  disjoint quarks moving with the same velocity) for several values of the wind rapidity  $\eta$ . The lower (higher) energy branch corresponds to the solution in Fig. 2 with lower (higher)  $\rho$ . The cusps where the two branches meet are at  $L = L_s$ .

where the last term is the contribution of the D5 brane to the energy.

In Fig. 3 we plot the energy of the baryon configurations at several values of  $\eta$ . As in Fig. 2, we see two configurations at every  $L < L_s$ . We have argued above that the higher energy configurations (those with the larger  $\rho$ ) are unstable, so we focus on the lower branch. We see that at  $\eta = 0$  this branch crosses zero energy at  $L = 0.073/T$ , whereas the largest  $L$  at which a baryon configuration can be found is  $L_s = 0.094/T$ . This means that for  $0.073 < LT < 0.094$ , even the lower branch solutions have become metastable, as they have more energy than  $N_c$  disjoint quarks. We see from Fig. 3 that this phenomenon does not occur at larger velocities; in fact, it arises only for  $\eta \leq 0.755$  since at  $\eta = 0.755$  the baryon configuration with  $L = L_s$  has the same energy as  $N_c$  disjoint quarks, i.e. zero energy in Fig. 3. At the low velocities  $\eta < 0.755$ , a more precise definition of the screening length would be to define it as the length at which the lower curve in Fig. 3 crosses zero. We see from Fig. 3 that by using  $L_s$  as our definition of the screening length at all velocities, as we do for simplicity, we are introducing only a small imprecision at low velocities,  $\eta < 0.755$ . These considerations have no effect on our calculation of  $L_s$  at large  $\eta$ , namely (3.11).

It is clear from (3.17) that in the large  $\eta$  limit (3.13) with  $\hat{L}$  held fixed and  $L$  therefore decreasing, the energy scales as  $-\sqrt{\cosh \eta}$ . This scaling can also be deduced from Fig. 3, as follows. The subtraction term (3.16) is defined such that for any given  $T$  and  $\eta$ , at small enough  $L$  the potential energy  $E(L)$  is the same as in vacuum (i.e. for  $T = \eta = 0$ ), namely  $E(L) \propto -1/L$ . And, if  $E \propto -1/L$  and the  $E(L)$  curves for different  $\eta$  overlap as seen in Fig. 3, then  $E$  must scale like

$-\sqrt{\cosh \eta}$  in the limit (3.13).

The baryon configuration that we have analyzed in this subsection is special in that all  $N_c$  strings are equivalent. In the next subsection we shall analyze a configuration for which this is not the case, for which we shall need the full formalism developed in Section 2.

### 3.2 Wind parallel to the baryon configuration

We now analyze the case where the  $N_c$  quarks are moving through the plasma (or, equivalently in their rest frame, feeling a hot wind blowing) in a direction parallel to their plane. We shall keep the wind blowing in the  $x_3$  direction as before, meaning that the boosted AdS black hole metric given by (2.3) is unchanged. We shall now put the  $N_c$  quarks in the  $(x_1, x_3)$ -plane.

With the quarks in the  $(x_1, x_3)$ -plane and the wind velocity in the  $x_3$  direction, the  $N_c$  strings in a circular baryon configuration are no longer equivalent, as the strings make different angles relative to the wind direction. The  $N_c$  strings would not all hit the D5-brane at the same angle in this case. Analyzing this case is possible, but we will instead consider a simpler configuration in which all  $N_c$  strings hit the D5-brane symmetrically. In terms of the formalism developed in Section 2, we choose a configuration in which the string density at the D5-brane is

$$\rho_V(s_1, s_2, s_3) = \frac{1}{\pi} \delta(s_1^2 + s_3^2 - s^2) \delta(s_2) , \quad (3.18)$$

where  $s$  is some constant and  $s_i = \partial_r x_i(r)|_{r_e}$ . The distribution (3.18) corresponds to requiring that the  $N_c$  strings hit the D5-brane with a uniform distribution in the azimuthal angle  $\phi$  in the  $(x_1, x_3)$ -plane and all with the same  $\partial_r x|_{r_e} = s$ . (Here,  $x \equiv \sqrt{x_1^2 + x_3^2}$ .) Unlike in the previous section, this specification of the baryon configuration in the vicinity of  $r = r_e$  will *not* correspond to having the  $N_c$  quarks at  $r = \infty$  arranged on a circle. Note that (3.18) guarantees that the net force exerted on the D5-brane in the  $x_1$ - and  $x_3$ -directions by the  $N_c$  quarks vanishes, meaning that (2.19), or equivalently (2.12), is automatically satisfied. Given the choices that we have made in specifying our baryon configuration, our task is twofold: we must determine  $s$  as a function of  $r_e$  such that the forces on the D5-brane in the  $r$ -direction due to gravity and due to the strings cancel; and, we must solve for the shape of the strings to determine what baryon configuration at  $r = \infty$  our choices correspond to.

The shape of each string is specified by two functions  $x_1(r)$  and  $x_3(r)$  that we must obtain. We shall find that, when projected onto the  $(x_1, x_3)$ -plane, the string worldsheets do not follow radial trajectories. That is, the trajectories  $x_1(r)$  and  $x_3(r)$  are not specified just by  $x(r)$ ; their azimuthal angle  $\phi$  is a nontrivial function of  $r$  also.

Applying equations (2.9) and (2.10) to (2.3) with nontrivial  $x_1(r)$  and  $x_3(r)$ , we find that

$$\mathcal{L}_{\text{string}} = \sqrt{A \left( \frac{1}{f(r)} + \frac{(x'_1)^2 r^2}{R^2} \right) + \frac{(x'_3)^2 r^2 f(r)}{R^2}} , \quad (3.19)$$

and find that the D5-brane action is given by (3.2) as before. With  $\mathcal{L}_{\text{string}}$  given by (3.19), the equations of motion (2.11) can be rearranged to give

$$x_1'^2 = \left( \frac{R^4}{r^2} \right) \left( \frac{K_1^2}{r^2 f A - R^2 K_3^2 A - R^2 K_1^2 f} \right), \quad (3.20)$$

$$x_3'^2 = \left( \frac{R^4}{f^2 r^2} \right) \left( \frac{K_3^2 A^2}{r^2 f A - R^2 K_3^2 A - R^2 K_1^2 f} \right). \quad (3.21)$$

Equation (2.13) for the balance of force in the radial direction becomes

$$\sum_{\text{strings}} \frac{R A / \sqrt{f}}{\sqrt{A (R^2 + f r^2 x_1'^2) + f^2 r^2 x_3'^2}} \Big|_{r_e} = N_c \Sigma(\rho, \eta), \quad (3.22)$$

where  $\Sigma(\rho, \eta)$  is as in (3.4) and is the downward gravitational force on the D5-brane and the left-hand side of (3.22) is the upward force due to the  $N_c$  strings. If we define  $\phi$  to be the azimuthal angle in the  $(x_1, x_3)$ -plane that a string makes at  $r = r_e$  where it connects to the D5-brane, defined such that  $\phi = 0$  ( $\phi = \pi/2$ ) is in the positive- $x_3$  (positive- $x_1$ ) direction, then our choice of having the  $N_c$  strings uniformly distributed in  $\phi$  turns the sum over strings in equation (3.22) into an integral over  $\phi$ ,

$$\sum_{\text{strings}} \rightarrow N_c \int_0^{2\pi} \frac{d\phi}{2\pi}, \quad (3.23)$$

and expression (3.22) becomes

$$\frac{R A}{\sqrt{f}} \int_0^{2\pi} \frac{d\phi}{2\pi} \frac{1}{\sqrt{A R^2 + s^2 f r^2 (A \sin^2 \phi + f \cos^2 \phi)}} \Big|_{r_e} = \Sigma(\rho, \eta), \quad (3.24)$$

where  $s = \partial_r x|_{r_e}$  was introduced in (3.18) and as before  $\rho \equiv r_0/r_e$ .

The constants  $K_1$  and  $K_3$  must be the same at any  $r$ . By evaluating (3.20) and (3.21) at  $r = r_e$  and rearranging, we determine that

$$K_1^2 = \frac{s^2 A^2 r^4 f \sin^2 \phi}{R^2 (A R^2 + s^2 r^2 f (A \sin^2 \phi + f \cos^2 \phi))} \Big|_{r_e}, \quad (3.25)$$

$$K_3^2 = \frac{s^2 r^4 f^3 \cos^2 \phi}{R^2 (A R^2 + s^2 r^2 f (A \sin^2 \phi + f \cos^2 \phi))} \Big|_{r_e}. \quad (3.26)$$

With these integration constants now determined, we can integrate Eqs. (3.20) and (3.21), obtaining

$$x_1(r) = \frac{\rho^3 R^4 K_1}{r_0^3} \int_1^{r/r_e} dy \frac{1}{\sqrt{Q}}, \quad (3.27)$$

and

$$x_3(r) = \frac{\rho^3 R^4 K_3}{r_0^3} \int_1^{r/r_e} dy \frac{y^4 - \rho^4 \cosh^2 \eta}{y^4 - \rho^4} \frac{1}{\sqrt{Q}}, \quad (3.28)$$

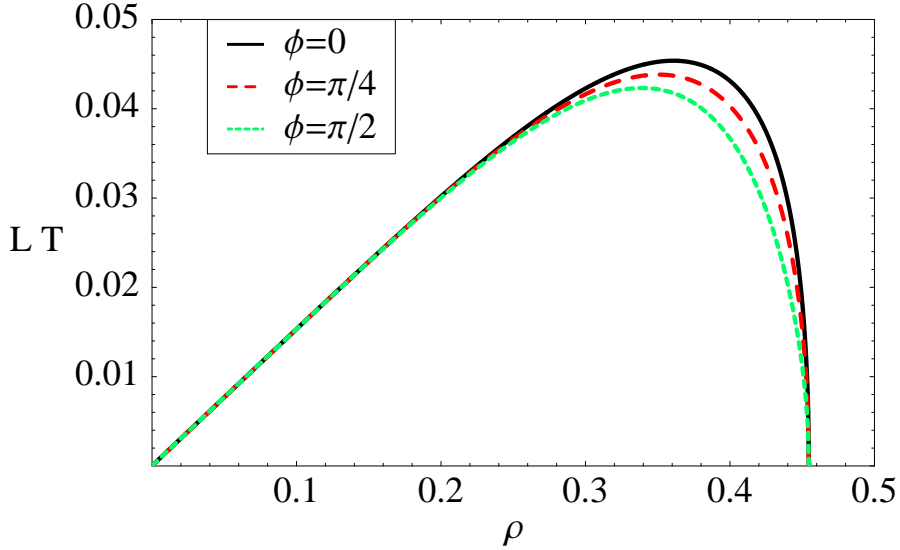


**Figure 4:**  $L$  versus  $\rho$  for strings oriented in the  $\phi = 0, \pi/4, \pi/2$  directions in the  $(x_1, x_3)$ -plane in a baryon configuration immersed in a plasma moving in the  $x_3$ -direction with rapidity  $\eta = 2$ . We see that at a given  $\rho$  the distance  $L$  in the  $(x_1, x_3)$ -plane between a quark and the D5-brane at the center of the baryon configuration depends on the angular position of the quark. This means that the  $N_c$  quarks do not lie on a circle.

where

$$Q \equiv (y^4 - \rho^4)(y^4 - \rho^4 \cosh^2 \eta) - \frac{R^4 \rho^4 K_1^2}{r_0^4} (y^4 - \rho^4) - \frac{R^4 \rho^4 K_3^2}{r_0^4} (y^4 - \rho^4 \cosh^2 \eta). \quad (3.29)$$

Equations (3.27) and (3.28) specify the shape of the string worldsheets, while  $r_e$  (equivalently,  $\rho$ ) is determined in terms of  $s$  by (3.24).

The calculation proceeds as follows. First, we solve (3.24) numerically to obtain the  $s$  required at a given  $\rho$ . Second, we pick a particular value of  $\phi$  and use  $s$  to evaluate (3.25) and (3.26), obtaining the  $r$ -independent, but  $\phi$ -dependent,  $K_1$  and  $K_3$ . Third, we evaluate (3.27) and (3.28) numerically, thus obtaining the shape of the string with a particular value of  $\phi$ . The position of the quark at  $r = \infty$  corresponding to this choice of  $\phi$  is then  $(x_1(\infty), x_3(\infty))$  and we can determine  $L = \sqrt{x_1(\infty)^2 + x_3(\infty)^2}$  for this choice of  $\phi$ . Fourth, we repeat the second and third steps for all values of  $\phi$ .

In Fig. 4 we show the  $L$  obtained as we have just described at three values of  $\phi$ , as a function of  $\rho$ . We conclude from the fact that  $L$  is different for different values of  $\phi$  that the  $N_c$  quarks at  $r = \infty$  are not arranged in a circle in the  $(x_1, x_3)$ -plane. We illustrate this explicitly in Figs. 5 and 6. We started with circularly symmetric boundary conditions at the D5-brane, but the resulting baryon configuration at the AdS boundary is “squashed”, wider in the direction of motion of the baryon and narrower in the perpendicular direction. Inspection of Fig. 4 or comparison of Figs. 5 and 6 shows that the shape of the baryon configuration at the AdS boundary changes with  $\rho$ , becoming more

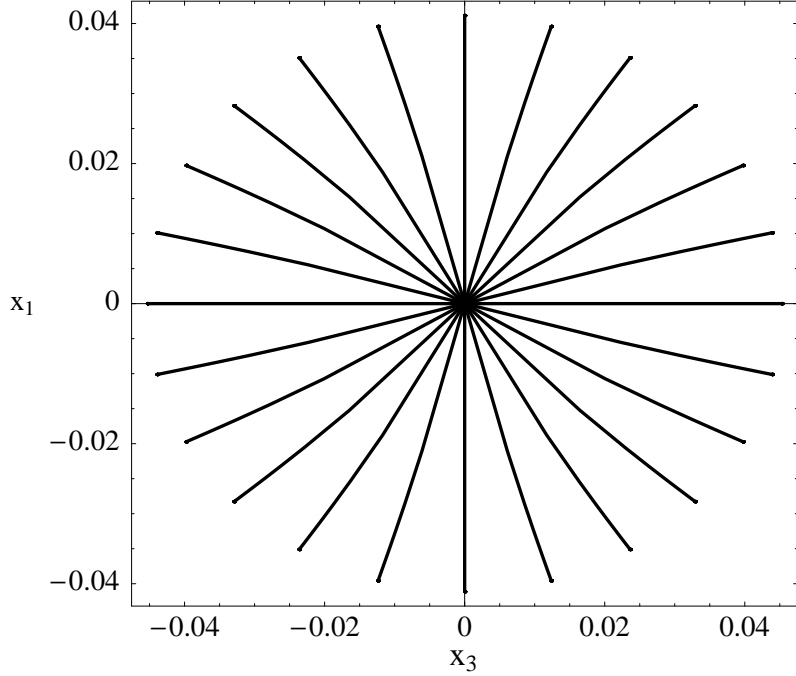


**Figure 5:** Strings projected on the AdS boundary for  $\eta = 2$  and  $\rho = 0.37$  for strings separated in  $\phi$  by  $\pi/12$ . (We have done all our calculations for  $N_c \rightarrow \infty$ , but have shown only 24 quarks in the figure.) Baryon motion is in the  $x_3$  direction. The figure is drawn in the rest frame of the baryon, meaning there is a hot wind in the  $x_3$  direction. The  $N_c$  quarks that make up the baryon configuration are not arranged in a circle: the ‘squashed circle’ is wider in the direction of motion. Note also that the projection of the strings are not straight lines.

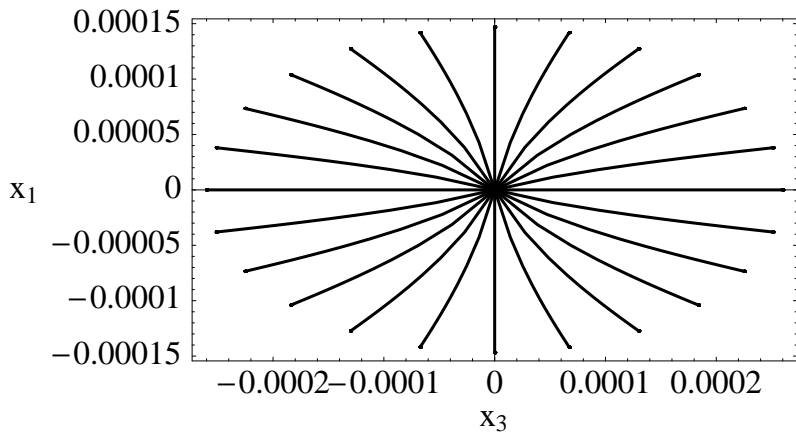


**Figure 6:** Same as Fig. 5, but for  $\rho = 0.4550611$ , very close to the maximum  $\rho$  at which a baryon configuration can be found at  $\eta = 2$ . This configuration is unstable, and has higher energy than the configurations with comparable  $L$ ’s at much lower  $\rho$ . However, it illustrates the ‘squashing’ of the baryon configuration away from a circular shape and the curvature of the projections of the strings onto the  $(x_1, x_3)$  plane. Both these effects are present in Fig. 5, but are more visible here.

squashed as  $\rho$  increases. In Figs. 5 and 6 we also see that the projections of the string worldsheets onto the  $(x_1, x_3)$ -plane are not straight radial lines. Their curved shapes are strikingly similar to the shapes of the projections of strings joining a static quark-antiquark in the meson configurations analyzed in Refs. [9, 10], although they are not precisely the same. Note that Eqs. (3.24)–(3.26) are symmetric in  $\phi \rightarrow \pi - \phi$ , which implies that string configurations are symmetric with respect to reflection in the  $x_1$  axis, i.e. under  $x_3 \rightarrow -x_3$ , as is manifest in Figs. 5 and 6. This forward-backward symmetry of the string configurations indicates that the baryon configuration feels no drag as it is moved through the plasma, just as for meson configurations [9–11], and as has been demonstrated previously for baryon configurations with zero size [33].

It is straightforward to compute the energy of the baryon configurations that we have found, as a function of  $\rho$ , but since (unlike in Section 3.1) the configurations are not characterized by a single  $L(\rho)$  there is no analogue of Fig. 3 here. Also, (again unlike when the wind blows perpendicular to the baryon configuration as in Section 3.1) we have no simple argument for at what  $\rho$  the baryon configurations in this section become unstable. Our argument in the previous section relied on the equivalence of all  $N_c$  strings, in that at a single  $\rho$  there was a change from “a deformation that increases  $\rho$  makes all  $N_c$  strings want to have larger  $L$ ” to “a deformation that increases  $\rho$  makes all  $N_c$  strings want to have smaller  $L$ ”. Here, we see from Fig. 4 that there is a range of  $\rho$  within which a deformation that increases  $\rho$  makes some strings want to have smaller  $L$  while other strings want to have larger  $L$ . Within this range of  $\rho$ , our simple argument yields no conclusion and a full stability analysis as in Refs. [29] is required. We leave this to future work.

The maxima of curves as in Fig. 4 define a screening length  $L_s$  for each  $\phi$  as a function of  $\eta$ . In Fig. 7 we plot  $L_s T \sqrt{\cosh \eta} = L_s T / (1 - v^2)^{1/4}$  versus  $\eta$  for different values of  $\phi$ . We find that the large- $\eta$  dependence of the screening length has the same form in all cases, namely

$$L_{s, \eta \gg 1} \propto \frac{1}{T \sqrt{\cosh \eta}} . \quad (3.30)$$

This is the same large  $\eta$  dependence found in Section 3.1, Eq. (3.11), and in mesons, Eq. (1.3). To make the former comparison manifest, in Fig. 7 we have also plotted  $L_s T \sqrt{\cosh \eta}$  for the case analyzed in Section 3.1 in which the wind velocity is perpendicular to the plane of the baryon configuration. When the wind velocity is parallel to the plane of the baryon configuration,  $L_s$  has a weak angular dependence. In particular, the constant of proportionality in Eq. (3.30) varies between 0.082 and 0.088 for different  $\phi$ , as can be seen in Fig. 7. A plot of  $L_s$  in the large  $\eta$  regime as a function of  $\phi$  is given in Fig. 8, which shows the smooth variation of  $L_s$  for large  $\eta$  as we change  $\phi$ . Note also that (3.30) is a good approximation all the way down to the small velocity limit  $\eta \rightarrow 0$ , since the proportionality constant in Eq. (3.30) merely changes from its ( $\phi$ -dependent) value at large  $\eta$  to the (obviously  $\phi$ -independent) value 0.094 at  $\eta = 0$ . The central conclusion to be drawn from Fig. 7, then, is that the simple velocity scaling (1.6) is a good approximation at all velocities and all angles.

The similarities between our results and those for the meson screening length go beyond just the dominant velocity scaling. Indeed, Fig. 7 is strikingly similar to Fig. 7 of Ref. [10]. There too, for the quark-antiquark case,  $L_s T \sqrt{\cosh \eta}$  is largest at  $\eta = 0$ , a few percent smaller for  $\eta \rightarrow \infty$  if the quark-antiquark dipole is oriented parallel to the wind, and a few percent smaller still if the

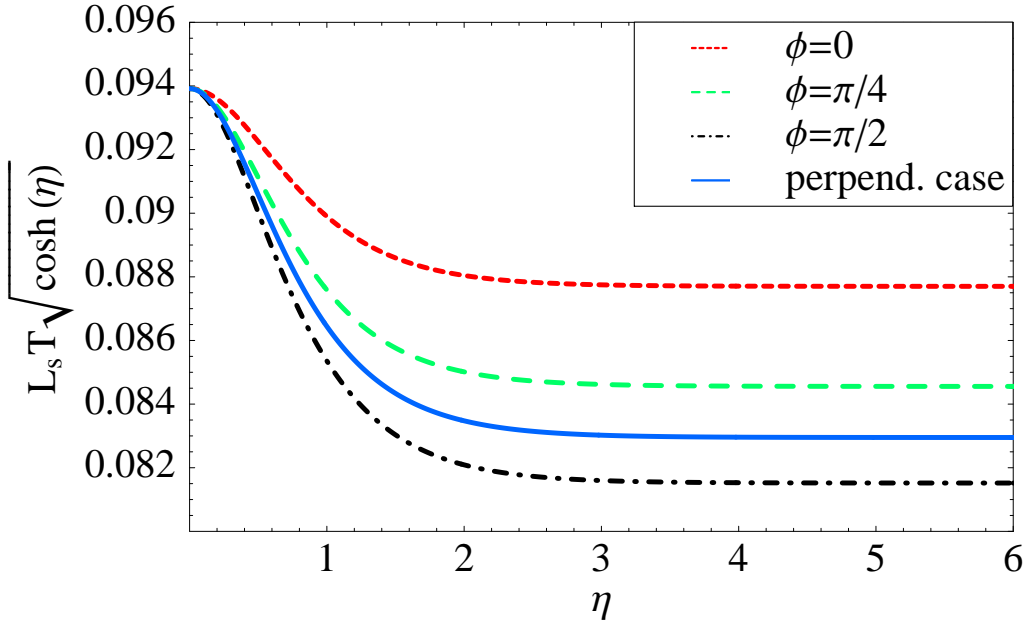


**Figure 7:** The screening length  $L_s$  as a function of  $\eta$  with its large- $\eta$  dependence  $\sqrt{\cosh \eta}$  scaled out. The solid curve is for the case of a wind velocity perpendicular to the plane of the baryon, as in Section 3.1. The other three curves are for wind velocity in the plane of the baryon, and show the  $L_s$  for the strings that make an angle  $\phi = 0, \pi/4, \pi/2$  with the direction of the wind.

dipole is oriented perpendicular to the wind. The only feature in our Fig. 7 that does not have a direct, almost quantitative, analogue in Ref. [10] is the *very* small difference between the curves for the two cases in which the wind direction is perpendicular to the line between the quark and the D5-brane, namely the case in which the wind is parallel to the plane of the baryon configuration and the quark is at  $\phi = \pi/2$  and the case in which the wind is perpendicular to the plane of the baryon configuration.

Although we have only done our analysis for a wind that is either perpendicular to or parallel to the plane of the baryon configuration, we expect that the qualitative features that we have found in this section should all be present for any wind direction except perpendicular.

In Subsections 3.1 and 3.2 we have analyzed two particular baryon configurations that suffice to make our point regarding the velocity dependence of baryon screening. The general formalism of Section 2 can straightforwardly be applied to baryon configurations with other shapes, whether specified by the density of quarks at infinity or the density of strings at the D5-brane vertex. Technically, in order to solve equations (2.12) and (2.13), it is simpler to specify the density of strings at the D5-brane as we have done in this subsection, but there is no obstacle of principle to analyzing arbitrary densities of quarks at infinity in any wind velocity. While the behavior at small  $\eta$  could differ for more general configurations, we expect that in the large  $\eta$  limit, the scaling behavior (3.30) should still apply. The formalism of Section 2 can also be used to generalize our results to the plasmas of other strongly coupled gauge theories. For example, following a line of

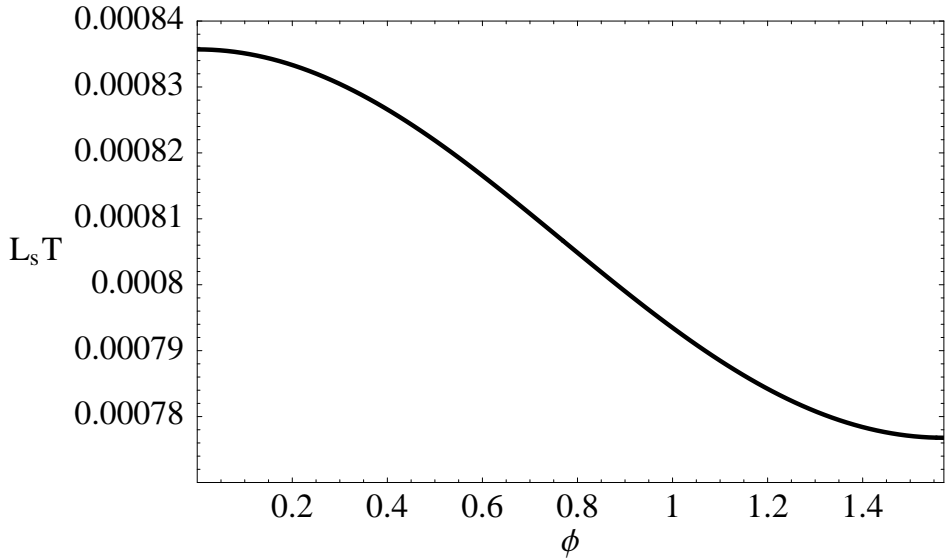


**Figure 8:** The screening length  $L_s$  as a function of  $\phi$  at a large value of  $\eta$ . Specifically,  $\eta = 10$  corresponding to  $\sqrt{\cosh \eta} = 1/(1 - v^2)^{1/4} = 104.9$ .

reasoning developed in Ref. [14] for the meson sector, it can be shown that in a certain class of gauge theories whose gravity duals are asymptotically AdS, as  $v \rightarrow 1$  the baryon screening length scales as  $L_s \propto (1 - v^2)^{1/4}/\varepsilon^{1/4}$ , where  $\varepsilon$  is the energy density of the plasma.  $\varepsilon$  is proportional to  $T^4$  for the specific theory that we have analyzed, at any  $v$ , in this Section.

## 4. Discussion

We have analyzed the screening of the static potential for a baryon configuration consisting of  $N_c$  quarks in a circle (or slightly squashed circle) moving with velocity  $v$  through the plasma of  $\mathcal{N} = 4$  SYM theory in a direction perpendicular (or parallel) to the plane of the configuration. We find a screening length

$$L_s = \frac{a(1 - v^2)^{1/4}}{T}, \quad (4.1)$$

where  $a$  depends only weakly on  $v$  and angles. For example,  $a = 0.094$  for  $v = 0$  while  $a = 0.083$  for  $v \rightarrow 1$  with the direction of motion perpendicular to the plane of the baryon configuration, and  $0.082 < a < 0.088$  for the case where the motion is parallel to the plane, again for  $v \rightarrow 1$ . In this last case,  $a$  is smallest for those quarks on the circle which are connected to the D5-brane junction at the center of the baryon by a string that is perpendicular to the direction of motion. The velocity dependence in (4.1) is precisely the same as that for the screening length defined by a quark and antiquark moving through the plasma, and even the weak angular dependence of  $a$  is strikingly similar. This is a confirmation of the robustness of the velocity dependence of screening that in the meson sector has as a consequence the experimentally testable prediction that in a range

of temperatures that is plausibly accessed in heavy ion collisions at RHIC (or at the LHC)  $J/\Psi$  (or  $\Upsilon$ ) suppression may set in only for quarkonia moving with a transverse momentum above some threshold [9]. In the baryon sector, it suggests that if baryons composed of three charm quarks are ever studied in heavy ion collision experiments which do not reach such high temperatures as to dissociate them at rest, their production could also be suppressed above some threshold transverse momentum.

We have found that if the baryon configuration we study feels a wind velocity parallel to its plane (and presumably at any direction except perpendicular) the  $N_c$  quarks are not all equivalent. Those in a direction perpendicular to the wind are most affected by the wind velocity, as in the configuration we analyze with azimuthally symmetric boundary conditions at the D5-brane they are the ones that are pulled in closest to the D5-brane and yet they are also the ones that have the smallest  $L_s$ . It is tempting to conclude from this that as a function of increasing  $v$  or  $T$  these quarks will dissociate first. However, justifying such a conclusion requires further work. It could be interesting to investigate configurations that are held circular in a wind parallel to their plane, which would no longer have azimuthally symmetric boundary conditions at the D5-brane. This would allow the analysis of a sequence of configurations with the same shape but different size rather than a sequence of configurations whose degree of squashing changes with size, as in our analysis. However, a definitive conclusion requires comparing the energies of a baryon configuration on the one hand with a well-separated quark and  $(N_c - 1)$ -quarks+D5-brane configuration, each trailing a dragging string, on the other hand. If the varying effectiveness of the screening of the potential binding different quarks to the baryon that we have found were to manifest itself as some quarks dissociating before others, as a function of increasing  $T$  or  $v$ , this would suggest that when heavy baryons with  $N_c = 3$  dissociate while moving through a strongly coupled plasma, they may at least initially dissociate into a quark and a diquark.

## Acknowledgments

We acknowledge helpful conversations with Wit Busza, Qudsia Ejaz, Tom Faulkner, Rob Myers, Gunther Roland, Aninda Sinha and Urs Wiedemann. HL is supported in part by the A. P. Sloan Foundation and the U.S. Department of Energy (DOE) OJI program. This research was supported in part by the DOE Offices of Nuclear and High Energy Physics under grants #DE-FG02-94ER40818 and #DE-FG02-05ER41360.

## References

- [1] J. M. Maldacena, *Adv. Theor. Math. Phys.* **2**, 231 (1998) [*Int. J. Theor. Phys.* **38**, 1113 (1999)] [[arXiv:hep-th/9711200](https://arxiv.org/abs/hep-th/9711200)]; E. Witten, *Adv. Theor. Math. Phys.* **2**, 253 (1998) [[arXiv:hep-th/9802150](https://arxiv.org/abs/hep-th/9802150)]; S. S. Gubser, I. R. Klebanov and A. M. Polyakov, *Phys. Lett. B* **428**, 105 (1998) [[arXiv:hep-th/9802109](https://arxiv.org/abs/hep-th/9802109)]; O. Aharony, S. S. Gubser, J. M. Maldacena, H. Ooguri and Y. Oz, *Phys. Rept.* **323**, 183 (2000) [[arXiv:hep-th/9905111](https://arxiv.org/abs/hep-th/9905111)].

- [2] S. J. Rey and J. T. Yee, Eur. Phys. J. C **22**, 379 (2001) [arXiv:hep-th/9803001].
- [3] J. M. Maldacena, Phys. Rev. Lett. **80**, 4859 (1998) [arXiv:hep-th/9803002].
- [4] S. J. Rey, S. Theisen and J. T. Yee, Nucl. Phys. B **527**, 171 (1998) [arXiv:hep-th/9803135]; A. Brandhuber, N. Itzhaki, J. Sonnenschein and S. Yankielowicz, Phys. Lett. B **434**, 36 (1998) [arXiv:hep-th/9803137]; J. Sonnenschein, arXiv:hep-th/0003032.
- [5] D. Bak, A. Karch and L. G. Yaffe, JHEP **0708**, 049 (2007) [arXiv:0705.0994 [hep-th]].
- [6] For a review, see F. Karsch, Nucl. Phys. A **783**, 13 (2007) [arXiv:hep-ph/0610024].
- [7] O. Kaczmarek and F. Zantow, Phys. Rev. D **71**, 114510 (2005) [arXiv:hep-lat/0503017].
- [8] O. Kaczmarek, F. Karsch, F. Zantow and P. Petreczky, Phys. Rev. D **70**, 074505 (2004) [Erratum-ibid. D **72**, 059903 (2005)] [arXiv:hep-lat/0406036].
- [9] H. Liu, K. Rajagopal and U. A. Wiedemann, Phys. Rev. Lett. **98**, 182301 (2007) [arXiv:hep-ph/0607062].
- [10] H. Liu, K. Rajagopal and U. A. Wiedemann, JHEP **0703**, 066 (2007) [arXiv:hep-ph/0612168].
- [11] K. Peeters, J. Sonnenschein and M. Zamaklar, Phys. Rev. D **74**, 106008 (2006) [arXiv:hep-th/0606195]; M. Chernicoff, J. A. Garcia and A. Guijosa, JHEP **0609**, 068 (2006) [arXiv:hep-th/0607089]; see also Appendix A of Ref. [12].
- [12] C. P. Herzog, A. Karch, P. Kovtun, C. Kozcaz and L. G. Yaffe, JHEP **0607**, 013 (2006) [arXiv:hep-th/0605158].
- [13] S. D. Avramis, K. Sfetsos and D. Zoakos, Phys. Rev. D **75**, 025009 (2007) [arXiv:hep-th/0609079].
- [14] E. Caceres, M. Natsuume and T. Okamura, JHEP **0610**, 011 (2006) [arXiv:hep-th/0607233].
- [15] M. Natsuume and T. Okamura, JHEP **0709**, 039 (2007) [arXiv:0706.0086 [hep-th]].
- [16] H. Dorn and T. H. Ngo, Phys. Lett. B **654**, 41 (2007) [arXiv:0707.2754 [hep-th]]; W. Y. Wen, arXiv:0708.2123 [hep-th]; T. Song, Y. Park, S. H. Lee and C. Y. Wong, Phys. Lett. B **659**, 621 (2008) [arXiv:0709.0794 [hep-ph]]; K. Peeters and M. Zamaklar, JHEP **0801**, 038 (2008) [arXiv:0711.3446 [hep-th]].
- [17] D. Mateos, R. C. Myers and R. M. Thomson, JHEP **0705**, 067 (2007) [arXiv:hep-th/0701132].
- [18] Q. J. Ejaz, T. Faulkner, H. Liu, K. Rajagopal and U. A. Wiedemann, arXiv:0712.0590 [hep-th].
- [19] A. Karch and E. Katz, JHEP **0206**, 043 (2002) [arXiv:hep-th/0205236]; M. Kruczenski, D. Mateos, R. C. Myers and D. J. Winters, JHEP **0307**, 049 (2003) [arXiv:hep-th/0304032]; J. Babington, J. Erdmenger, N. J. Evans, Z. Guralnik and I. Kirsch, Phys. Rev. D **69**, 066007 (2004) [arXiv:hep-th/0306018]; M. Kruczenski, D. Mateos, R. C. Myers and D. J. Winters, JHEP **0405**, 041 (2004) [arXiv:hep-th/0311270].

[20] R. Sommer and J. Wosiek, Nucl. Phys. B **267**, 531 (1986); G. S. Bali, Phys. Rept. **343**, 1 (2001) [arXiv:hep-ph/0001312]; T. T. Takahashi, H. Matsufuru, Y. Nemoto and H. Suganuma, Phys. Rev. Lett. **86**, 18 (2001) [arXiv:hep-lat/0006005]; C. Alexandrou, P. De Forcrand and A. Tsapalis, Phys. Rev. D **65**, 054503 (2002) [arXiv:hep-lat/0107006]; C. Alexandrou, P. de Forcrand and A. Tsapalis, Nucl. Phys. Proc. Suppl. **109A**, 153 (2002) [arXiv:nucl-th/0111046]; T. T. Takahashi, H. Suganuma, Y. Nemoto and H. Matsufuru, Phys. Rev. D **65**, 114509 (2002) [arXiv:hep-lat/0204011]; C. Alexandrou, P. de Forcrand and O. Jahn, Nucl. Phys. Proc. Suppl. **119**, 667 (2003) [arXiv:hep-lat/0209062]; O. Jahn and P. de Forcrand, Nucl. Phys. Proc. Suppl. **129**, 700 (2004) [arXiv:hep-lat/0309115]; T. T. Takahashi and H. Suganuma, Phys. Rev. D **70**, 074506 (2004) [arXiv:hep-lat/0409105]; Ph. de Forcrand and O. Jahn, Nucl. Phys. A **755**, 475 (2005) [arXiv:hep-ph/0502039].

[21] K. Hubner, F. Karsch, O. Kaczmarek and O. Vogt, arXiv:0710.5147 [hep-lat].

[22] E. Witten, JHEP **9807**, 006 (1998) [arXiv:hep-th/9805112].

[23] D. J. Gross and H. Ooguri, Phys. Rev. D **58**, 106002 (1998) [arXiv:hep-th/9805129].

[24] A. Brandhuber, N. Itzhaki, J. Sonnenschein and S. Yankielowicz, JHEP **9807**, 020 (1998) [arXiv:hep-th/9806158].

[25] Y. Imamura, Nucl. Phys. B **537**, 184 (1999) [arXiv:hep-th/9807179]; C. G. Callan, A. Guijosa and K. G. Savvidy, Nucl. Phys. B **547**, 127 (1999) [arXiv:hep-th/9810092]; B. Craps, J. Gomis, D. Mateos and A. Van Proeyen, JHEP **9904**, 004 (1999) [arXiv:hep-th/9901060]; C. G. Callan, A. Guijosa, K. G. Savvidy and O. Tafjord, Nucl. Phys. B **555**, 183 (1999) [arXiv:hep-th/9902197]; J. Gomis, A. V. Ramallo, J. Simon and P. K. Townsend, JHEP **9911**, 019 (1999) [arXiv:hep-th/9907022].

[26] G. C. Rossi and G. Veneziano, Nucl. Phys. B **123**, 507 (1977); B. Z. Kopeliovich and B. G. Zakharov, Z. Phys. C **43**, 241 (1989); D. Kharzeev, Phys. Lett. B **378**, 238 (1996) [arXiv:nucl-th/9602027]; M. Gyulassy, V. Topor Pop and S. E. Vance, Heavy Ion Phys. **5**, 299 (1997) [arXiv:nucl-th/9706048]; H. W. Fricke and C. C. Noack, Phys. Rev. Lett. **80**, 3014 (1998) [arXiv:hep-ph/9711389]; S. E. Vance, M. Gyulassy and X. N. Wang, Phys. Lett. B **443**, 45 (1998) [arXiv:nucl-th/9806008]; B. Kopeliovich and B. Povh, Phys. Lett. B **446**, 321 (1999) [arXiv:hep-ph/9810530]; S. E. Vance and M. Gyulassy, Phys. Rev. Lett. **83**, 1735 (1999) [arXiv:nucl-th/9901009]; I. Vitev and M. Gyulassy, Phys. Rev. C **65**, 041902 (2002) [arXiv:nucl-th/0104066]; G. H. Arakelian, A. Capella, A. B. Kaidalov and Yu. M. Shabelski, Eur. Phys. J. C **26**, 81 (2002); V. T. Pop, M. Gyulassy, J. Barrette, C. Gale, X. N. Wang and N. Xu, Phys. Rev. C **70**, 064906 (2004) [arXiv:nucl-th/0407095];

[27] L. Susskind and E. Witten, arXiv:hep-th/9805114; A. W. Peet and J. Polchinski, Phys. Rev. D **59**, 065011 (1999) [arXiv:hep-th/9809022].

[28] M. C. Chu and T. Matsui, Phys. Rev. D **39**, 1892 (1989).

[29] J. J. Friess, S. S. Gubser, G. Michalogiorgakis and S. S. Pufu, JHEP **0704**, 079 (2007) [arXiv:hep-th/0609137]; S. D. Avramis, K. Sfetsos and K. Siampos, Nucl. Phys. B **769**, 44 (2007) [arXiv:hep-th/0612139]; S. D. Avramis, K. Sfetsos and K. Siampos, arXiv:0706.2655 [hep-th].

- [30] F. Karsch, E. Laermann and A. Peikert, Phys. Lett. B **478**, 447 (2000) [arXiv:hep-lat/0002003];  
F. Karsch, Nucl. Phys. A **698**, 199 (2002) [arXiv:hep-ph/0103314].
- [31] A. Sinha, talk at Quark Matter 2008, February 2008, Jaipur, India; R. Myers and A. Sinha, private communication.
- [32] S. S. Gubser, Phys. Rev. D **74**, 126005 (2006) [arXiv:hep-th/0605182];
- [33] M. Chernicoff and A. Guijosa, JHEP **02**, 084 (2007) [arXiv:hep-th/0611155].